Gamma Ray Spectrometer Upgrade
(GSU)

COMMISSIONING REPORT

- deliverable D40 -

T. Craciunescu[1], V. Braic[1], P. Brown[4], A. Brosławski[2], N. Cruz[5], A. Čufar[3], D. Croft[4], M. Curuia[1], S. Dorling[4], A. Fernandes[5], L. Giacomelli[6], V. Goloborod'ko[7], G. Gorini[6], S. Griph[4], V. Kiptily[4], I. Kodeli[3], S.Korolczuk[2], I. Lengar[3], R. Lucock[4,] R. Naish[4], M. Nocente[6], R. C. Pereira[5], K. Schoepf[7], B. Santos[5], L. Snoj[3], S. Soare[1], M. Tardocchi[6], A. Urban [2,] V.L. Zoita[1], I. Zychor [2]

EUROfusion Consortium, JET, Culham Science Centre, Abingdon, OX14 3DB, UK

[1]Institute of Atomic Physics, Bucharest, Romania

[2]National Centre for Nuclear Research, Warsaw, Poland

[3]Slovenian Fusion Association (SFA), Jozef Stefan Institute, Reactor Physics Department, Ljubljana, Slovenia

[4]CCFE, Culham Science Centre, Abingdon, United Kingdom

[5]Instituto de Plasmas e Fusão Nuclear, Instituto Superior Técnico, Universidade de Lisboa

[6]Instituto di Fisica del Plasma "Piero Caldirola«, Consiglio Nazionale delle Ricerche, Milano, Italy

[7]University of Innsbruck, Fusion@Österreichische Akademie der Wissenschaften, Austria

1. Introduction

The α-particles produced by the nuclear fusion reactions between deuterons and tritons will provide the power for self-sustained DT-plasma burn by transferring their energy to the thermal plasma during their slowing down. Therefore the adequate confinement of α-particles will be essential to provide efficient heating of the bulk plasma and steady-state burning of reactor plasma. Consequently, the investigation of α-particles behaviour for deciphering the main mechanisms of their slowing down, redistribution and losses, appear as priority task for the planned deuterium- tritium experiments on JET in order to develop optimal plasma scenarios [1].

On JET the α-particle diagnostic is based on the nuclear reaction $^{9}Be(\alpha,n\gamma)^{12}C$ between confined α-particles and beryllium impurity ions typically present in the plasma [2-3]. The applicability of gamma-ray diagnostics is strongly dependent on the fulfilment of rather strict requirements for the definition and characterization of the neutron and gamma radiation fields (detector Field-of-View, radiation shielding and attenuation, parasitic gamma-ray sources). For operating this diagnostic at the high DT neutron fluxes expected in the future high-power DT campaign on JET, specific improvements are needed in order to provide good quality measurements in the D-T campaign, characterized by a more challenging radiation environment. Obtaining a high energy resolution of the spectra and making the system compatible with high count rate signal processing were the main objectives of the upgrading of the tangential gamma-ray spectrometer.

In order to accomplish these objectives, the inclusion or upgrade of several components was necessary:

- **<u>The Radiation Field Assembly (RFCA)</u>**

  A radiation field components assembly, allowing the definition and control of the neutron and gamma-ray radiation fields along the full line-of-sight of the KM6T gamma-ray spectrometer, has been designed, manufactured and installed. RFCA allows the definition of the spectrometer Field-of–View (FoV) across the DT plasma and provides adequate shielding of the gamma-ray detector from parasitic neutron and gamma-ray sources. The main component of RFCA is the LiH neutron attenuator (NA). LiH material has the advantage of avoiding carbon-containing materials which lead to the production of inelastic scattering neutrons with energies E>5 MeV from $^{12}C(n,n'\gamma)^{12}C$ reactions and, consequently, to an unwelcome background of 4.44 MeV γ–rays. LiH with a natural Li composition is compact, effective and well transparent to MeV γ-rays. RFCA contains a Movable Gamma-Ray Shield (MGRS), and a Fixed Gamma-Ray Shield (FGRS). Depending on the position of MGRS the system attenuation is setup for DT or DD experiments. A third position of MGRS allows it to work as a gamma-ray shutter.

- **<u>The Detectors and Data Acquisition System</u>**

  As in the DT experiments the gamma-ray detector must fulfil requirements for high count rate measurements, the old BGO-detector has been replaced with new detector modules (detector module 1 (DM1) based on LaBr3 scintillator and detector module 2 (DM2) based on CeBr3 scintillator) and an associated digital data acquisition system (DAQ).

  The new scintillators are characterized by short decay times (~20ns) and a high photons yields. The coupling of the scintillators with photomultiplier tubes in specially designed detector modules allows high count rates, over 2MHz. The high rate capability is enabled by a dedicated pulse digitization system with a nominal 14-bit resolution.

A. RFCA Commissioning

The Radiation Field Components Assembly (RFCA) has the following main components, from the plasma to the detector:

- Two tandem collimators which define the spectrometer filed-of-view inside the JET plasma. The tandem collimators, Fig. A-1, are provided with additional collimator modules in order to fulfil the requirements for DT operation;

- Two gamma-ray shields: a Movable Gamma-Ray Shield (MGRS), and a Fixed Gamma-Ray Shield (FGRS), Fig. A-2 for minimizing the flux of parasitic gamma radiation reaching the detector.

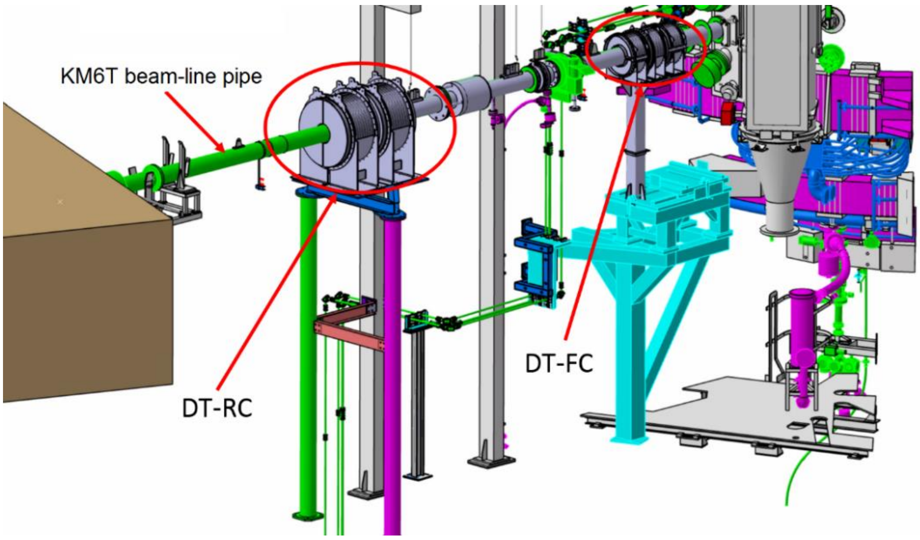

Fig. A-1. Upgraded KM6T tandem collimators. DT-FC: Front Collimator for DT pulses. DT-RC: Rear Collimator for DT pulses.

The gamma-ray shields are positioned inside a bunker on the south wall of the JET experimental hall, behind an X-ray spectrometer chamber (KX1 spectrometer, in Fig. A-2).

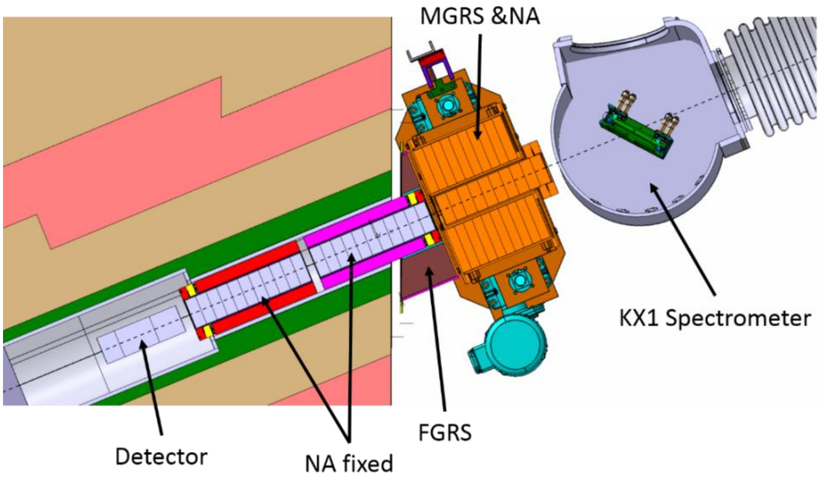

Fig. A-2 Radiation Field Components Assembly at the detector end of the KM6T beam-line. MGRS: Movable Gamma-Ray Shield; FGRS: Fixed Gamma-Ray Shield; NA: Neutron Attenuator

A first gamma-ray shield is vertically movable with three working positions, while a second shield is bolted onto a metal sheet placed on the vertical bunker wall. For the MGRS the materials of choice were stainless-steel (SS 304) metal sheet for the casings and slabs of nuclear grade lead for the shielding material. The two lids which close the movable shield assembly are also made of SS metal sheet. The casing structure is reinforced by two SS rings welded to it towards both ends. The casing elements are bolted. The shield is securely fixed to a cradle which is bolted to a U-channel that transfers the load to an electro-mechanical driver system. The vertical movement is driven by a jack system powered by an electric motor, Fig. A-3.

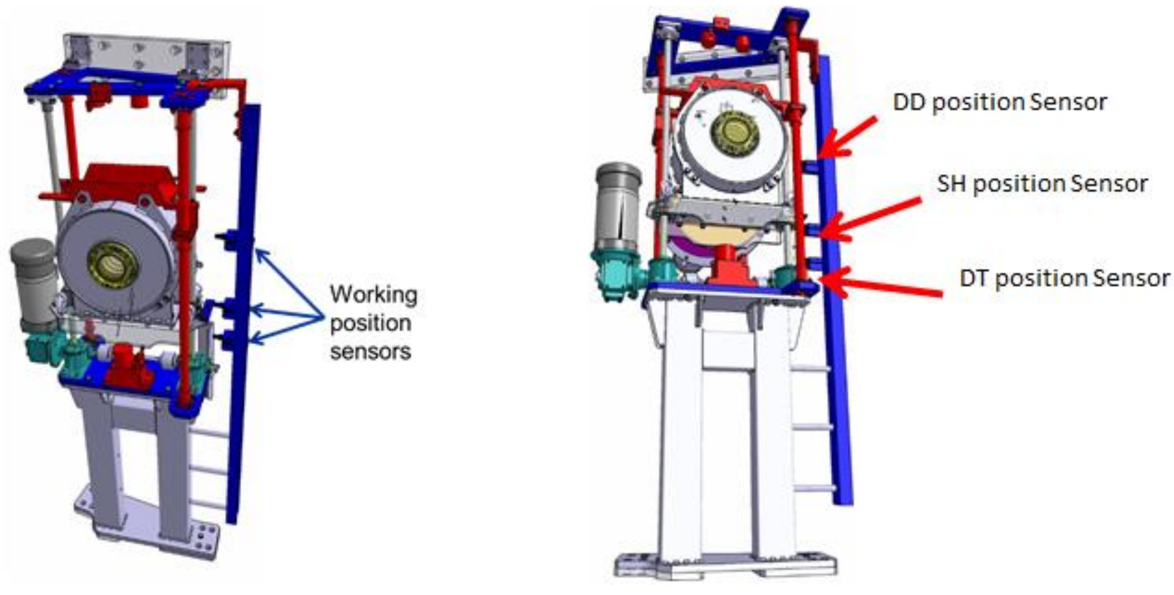

Fig. A-3 Movable Gamma-Ray Shield (MGRS) working positions: lower position for DT discharges; middle position for gamma-ray shutter; top position for DD discharges.

The electrical motor and movable shield assembly is supported by a frame fixed onto the bunker wall and floor. The electric motor is fitted with brake that is active when the motor is not powered. MGRS has the following working positions and corresponding functions (Fig. A-3):

-Bottom: maximum neutron attenuation thickness, for DT discharges;

-Middle: middle working position, for gamma-ray Shutter;

-Top: minimum attenuation thickness, for DD discharges.

MGRS has to be moved to the top or to the bottom positions as required by experiments. MGRS in its middle position is to be used as a gamma-ray shutter for the measurement of the gamma-ray background at the detector location during a JET pulse.

1. MGRS Control

The MGRS can be locally controlled by means of KM6T Control Unit and monitored by the JET COntrol and Data Acquisition System (CODAS), Fig. A-4.

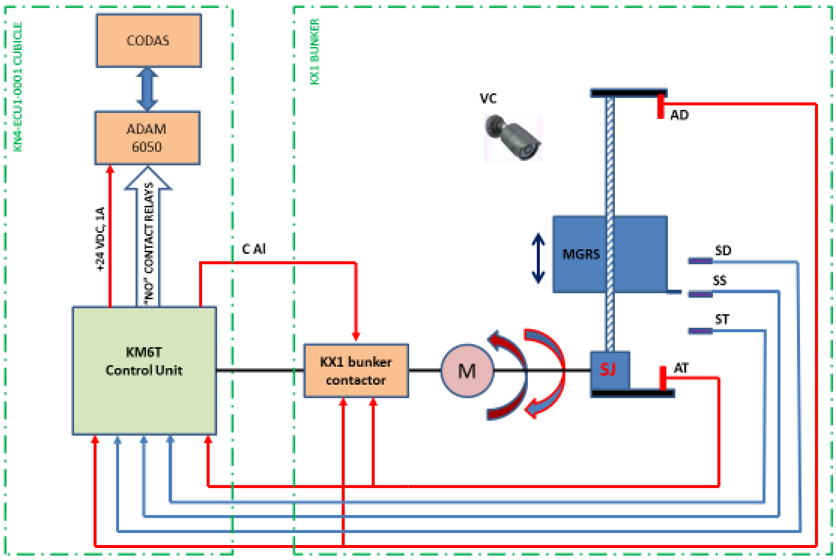

M -3 phases AC motor, 0.485 kW, with brake; SJ- screw jacks; MGRS-mobile gamma ray shield; AT/AD-safety limit switches for alarm in DT/DD positions; SD/SS/ST-limit switches for working positions; VC- video camera; C Al- Cancel alarm

Fig. A-4 Movable Gamma-Ray Shield (MGRS) command and control. PLC: Programmable Logic Controller; Eth: Ethernet connection; CODAS: COntrol and Data Acquisition System

KM6T Control Unit is designed with a classic scheme consisting of relays, electric buttons switches and contactors. The connection with CODAS is done by means of dedicated interface ADAM 6050. The working positions of the shield are known using three limit switches: ST - switch Tritium, SS – switch Shutter and SD - switch Deuterium. Another two limit switches are used in case when the shield will overshoot the working positions: AT – alarm for DT position and AD – alarm for DD position. Timer relays are controlling the displacement times of the MGRS and stop the electric motor when the preset values are exceeded. There are also two protections on the motor current, a current sensor switch that cuts the current through motor when instant current exceeds the pre-set value, and a thermal circuit breaker. The current sensor switch works faster than thermal circuit breaker. A video camera placed into the KX1 bunker is used to witness all movements of MGRS. The video camera (VC) is connected direct to the computer via an UTP cable.

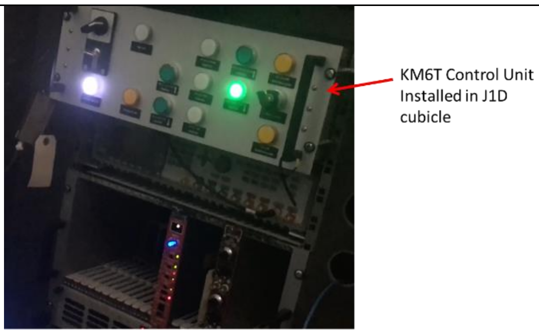

Fig. A-5 Front view of KM6T Control Unit installed within KN4-ECU1-0001 CUBICLE

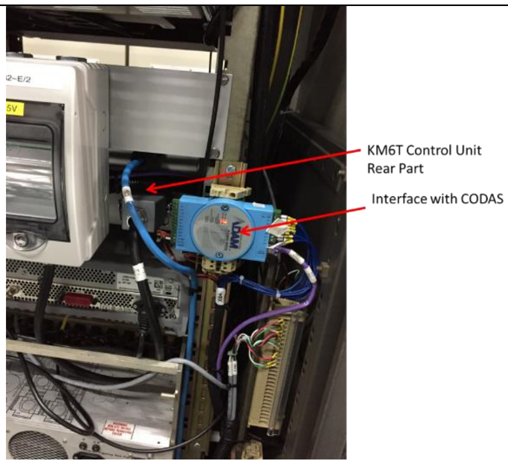

Fig. A-6 Rear view of KN4-ECU1-0001 CUBICLE with KM6T Control Unit and CODAS interface

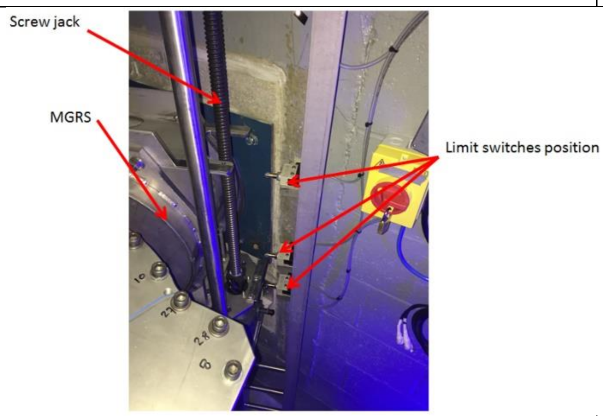

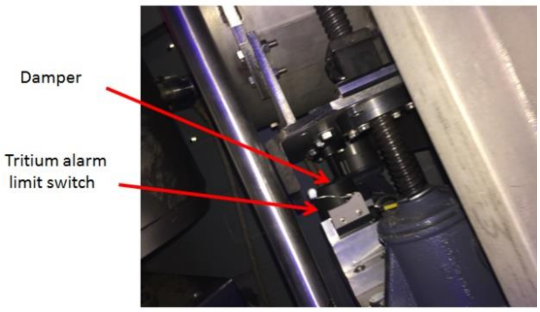

Fig. A-7 Installed components inside the KX1 Bunker	*Fig. A-8 Alarm Limit Switch and damper for DT position*
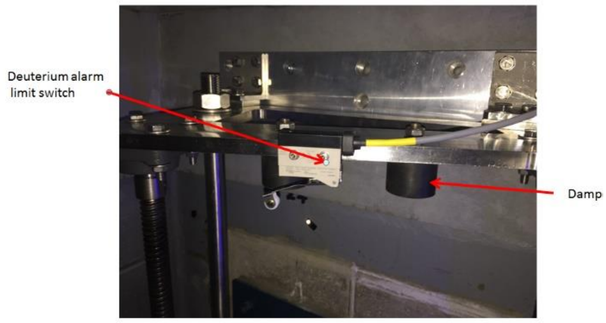	
Fig. A-9 Alarm Limit Switch and dampers for DD position	*Fig. A-10 Video camera to witness MGRS movements*

4. MGRS Commissioning

As part of RFCA, MGRS is to be moved to the top or to the bottom positions as required by experiments. MGRS in its middle position is to be used as a gamma-ray shutter for the measurement of the gamma-ray background at the detector location during a JET pulse.

Based on information received from position switches the KM6T Control Unit supply electrical motor that drives the two screw jacks to move the mobile shield.

The commissioning activities have been split in two parts:

4.1 Commissioning of the bunker components

During this stage the following, inside the KX1 bunker, were checked or done:

- The positioning of limit switches for working position;
- The positioning of alarm switches used to cut the movement of MGRS in case when the working position has been overshot;
- The positioning of the tandem damper alarm limit switches to act efficiently in case of MGRS overshot the alarm position;
- The functionality of video camera, that it has been connected to laptop;
- The electric motor has been driven by an electrical screw driver and the functionality of limit switches has been checked. Pictures with MGRS in working position, taken from the display of the laptop, are presented in Fig. A-11 (DT), Fig. A-12(SH), Fig. A-13(DD);

Fig. A-11 MGRS in DT working position

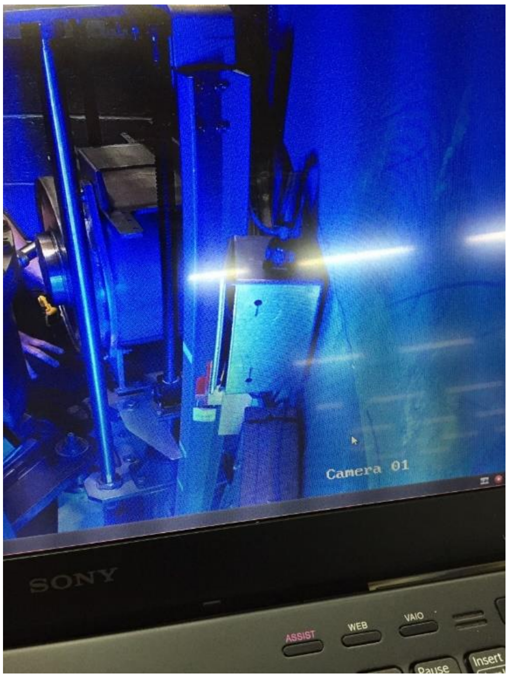

Fig. A-12 MGRS in SH working position

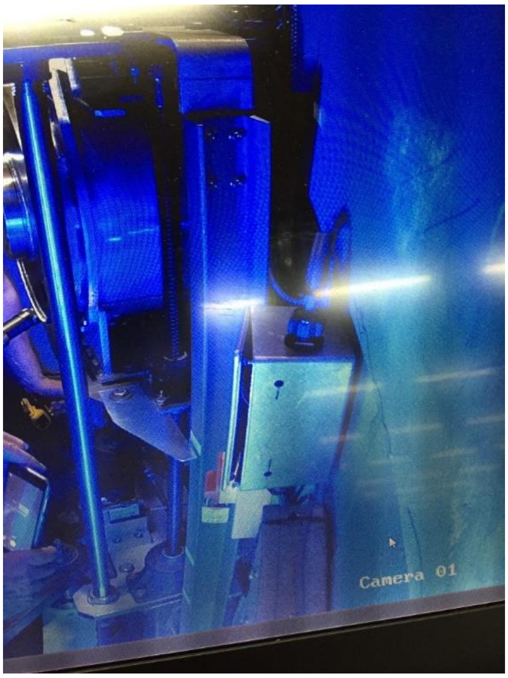

Fig. A-13 MGRS in DD working position

4.2 Commissioning of the full system – KM6T Control Unit and bunker components

Having all bunker components installed and KM6T Control Unit installed within the J1D Cubicle, as it is shown in the Fig. A-5 and Fig. A-6, the following were done and witnessed by video camera.

- Movements of MGRS to check if the working positions are reached;
- Setting of timer relays to have a real Time Out protection. The following values have been set:
    - DT to SH movement: 28 s;
    - SH to DD movement: 58 s;
    - DD to SH movement: 58 s;
    - SH to DT movement: 28 s.
- Movement of MGRS to check if the alarm limit switches are working. For this action corresponding limit switches have been cancelled.
- The connection with CODAS has been checked and all signals have been read.
    - 1. KM6T Control Unit status
    - 2. Movable shield in DT position
    - 3. Movable shield in SH position
    - 4. Movable shield in DD position
    - 5. Movable shield in DT alarm position
    - 6. Movable shield in DD alarm position
    - 7. Movement time out
    - 8. Motor overload
- Pictures regarding the commissioning of the MGRS full system are presented in Figs. A-14-20.

	F *Fig. A-14 MGRS in SH position, to be moved to DD working position*
	*Fig. A-15 MGRS in movement from SH to DD working position*
	*Fig. A-16 MGRS in DD position*
	*Fig. A-17 MGRS in movement from DD to SH working position*

	*Fig. A-18 MGRS in SH working position*
	*Fig. A-19 MGRS in movement from SH to DT working position*
	*Fig. A-20 MGRS in DT working position*

B. Detectors and Data Acquisition System Commissioning

B.1 DAQ Commissioning

DAQ aims to acquire and process in real-time the signals provided by the new LaBr3 and CeBr3 based detectors. The DAQ application software that runs on top of Scientific Linux OS is composed by: i) hardware drivers; ii) MARTe real-time framework application (acquisition control and CODAS interface); iii) data analysis codes and tools. During DAQ commissioning maintenance and corrections were made to the codes of the MARTe real-time framework application as well as new developments to the MARTe real-time framework application and to the data analysis codes and tools. DAQ is operated by dedicated codes, capable of acquiring the signals at full rate, and simultaneously processing them in real-time through suitable algorithms.

The KM6T spectrometer has been operated continuously to check for the system robustness as well as calibration consistency. These tests consisted in 10 runs of 12 hours and they used Na22 and Cs137 + Ba137 calibration sources.

In order to check the baseline fluctuation with the increasing event rate due to the ac-coupling of the digitizer, a test procedure based on the acquisition in raw mode from a signal generator with increasing event rate: 1, 5, 10 and 20 MHz has been used. Figs. B1.1-1 to B1.1-4 show 1024 samples of a raw acquisition at 200 MHz.

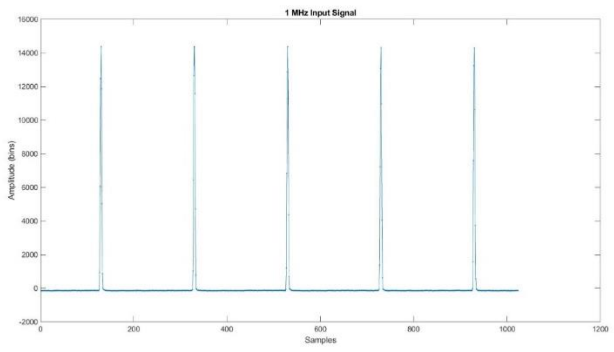

Figure B1.1-1: 1 MHz input signal. 1024 samples

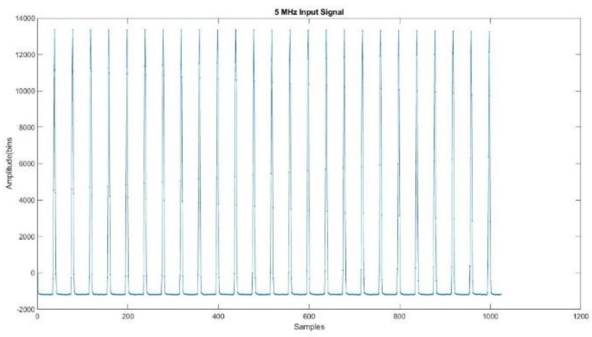

Figure B1.1-2: 5 MHz input signal. 1024 samples

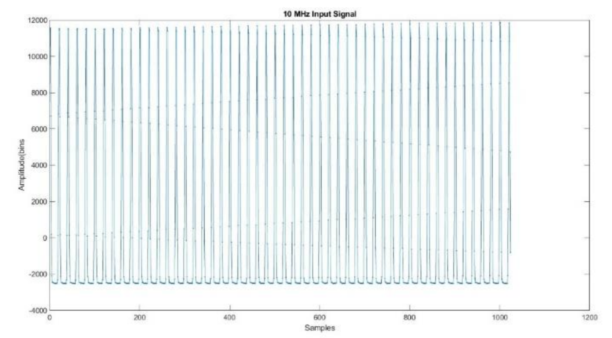

Figure B1.1-3:10 MHz input signal. 1024 samples.

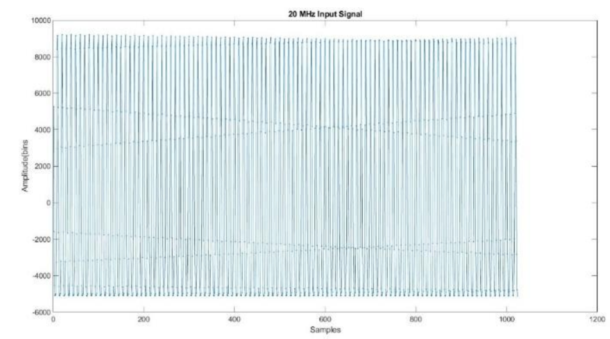

Figure B1.1-4:20 MHz input signal. 1024 samples.

The signals acquired in raw mode were processed in order to obtain a spectrum, which, ideally is a sharp energy peak. Table B.1-1 and Fig. B1.1-5 depict the results obtained.

Table 1: Results for the KM6T spectrometer.

Input	Agilent Generator (900 mV)			amplitude (V)		
Freq (MHZ)	nº of pulses	max time	event rate	min volt	max volt	voltage range
1	320084	0.32	1000262.5	-0.012047313	0.904552424	0.916599737
5	1600420	0.32	5001312.5	-0.077303592	0.839798116	0.917101708
10	3200789	0.32	10002465.63	-0.16012887	0.755466925	0.915595794
20	6401682	0.32	20005256.25	-0.322767596	0.591824255	0.914591852

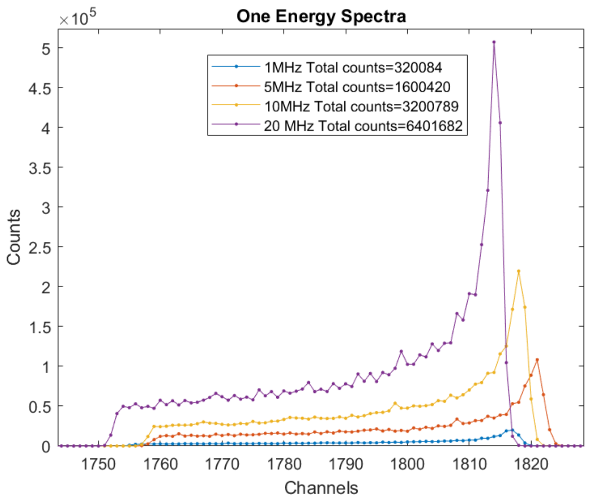

Figure B1.1-5: A signal generator from Agilent had been settled to produce a narrow pulse with several frequencies 1, 5 10 and 20 MHz. These signals were acquired in raw in the KM6T acquiring channel and processed in order to obtain a spectrum.

B.2 Detectors commissioning

The upgraded KM6T system comprises a set of two detectors based on LaBr3/CeBr3 scintillator crystals each coupled to a photomultiplier tube (PMT) which guarantee good energy resolution and high count rate capabilities. These features are essential for a successful gamma-ray spectroscopy in the harsh neutron-gamma mix environment of the forthcoming deuterium-tritium campaign.

The 3”x6” LaBr3 scintillator crystal, provided by Saint-Gobain, is coupled to a Hamamatsu photomultiplier tube (PMT) equipped with an active base. The active components are necessary to sustain the high rate burst events. The 3”×3” cylindrical CeBr3 scintillator is encapsulated in a 0.5 mm thick Al housing and coupled to a R6233-100 PMT. It is equipped with a SMA connector for tests with LED sources.

The LaBr3 detector has been installed in 2018 and it has been used routinely during the C38 campaign. It has been commissioned in ^{3}He ion ICRH experiments at JET.

A first round of experiments was performed in August 2019 (M18-11, SC: Yevgen Kazakov), while the second round of experiments was performed in October (M18-11, SC: Y. Kazakov and M18-12, SC: M. Nocente). In these experiments, MeV range deuterium ions were generated by coupling radio-frequency waves to a beam of deuterons in a mixed deuterium-^{3}He plasma with relative concentrations of about 70% and 30%, respectively. As a result, we expect gamma-rays from d+^{9}Be reactions. Besides, as the plasma also produces fusion born alpha particles from the d+^{3}He fusion reaction, we expect gamma-ray peaks from the α+^{9}Be reaction.

Fig. B.2-1 shows a gamma-ray spectrum collected by the KM6T detector in these experiments compared with the gamma-ray spectrum collected by the KM6S detector in the same scenario (Fig. B.2-2). Unlike the KM6T instrument, which has a horizontal line of sight, KM6S views the plasma along a vertical line of sight that roughly covers the radial region R=2.7 m to R=3.1 m.

In both spectra we observe clear peaks at 2.86 MeV, 3.37 MeV and 3.59 MeV, which are born from the d+^{9}Be reaction between deuterons accelerated by ICRH and naturally found ^{9}Be impurities. In particular, the observation of these peaks indicate that deuterons must have energies exceeding 500 keV. The same peaks are also observed by KM6S, with comparable intensities. The production of a population of deuterons with energy exceeding 500 keV is also independently confirmed by the neutron spectrum measured with the TOFOR (KM11) instrument.

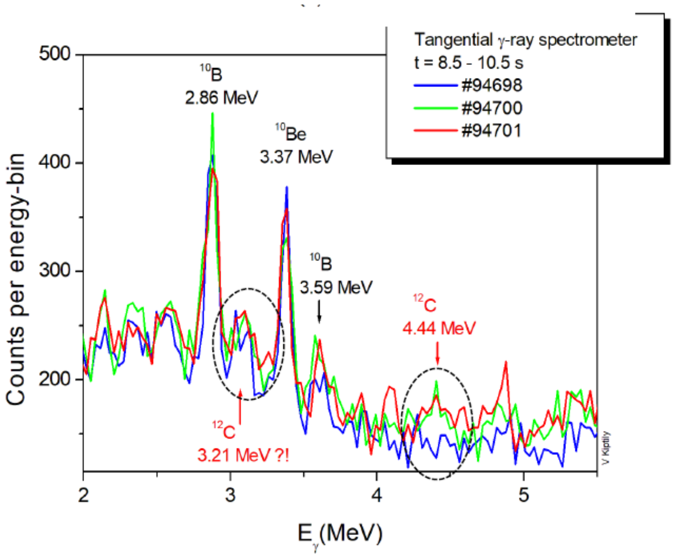

Figure B.2-1: gamma-ray spectrum from the KM6T horizontal gamma-ray spectrometer developed by the GSU project and measured in JET discharges #94698, 94700 and 94701 from the 3 ion ICRH experiment M18-11.

In the KM6T spectrum we also observe peaks at 4.44 MeV and 3.21 MeV born from the α+^{9}Be reaction between fusion born alpha particles and ^{9}Be impurities. The intensity of these peaks is however larger for the KM6S detector compared with KM6T. The reason is that the KM6T line of sight is about 20 cm below the position of the magnetic axis in these experiments and thus misses the very core of the plasma, where fusion alpha particles are predominantly born. On the other hand, the KM6S line of sight fully covers the plasma core and is better suited at measuring gamma-rays induced by fusion born alpha particles in this scenario.

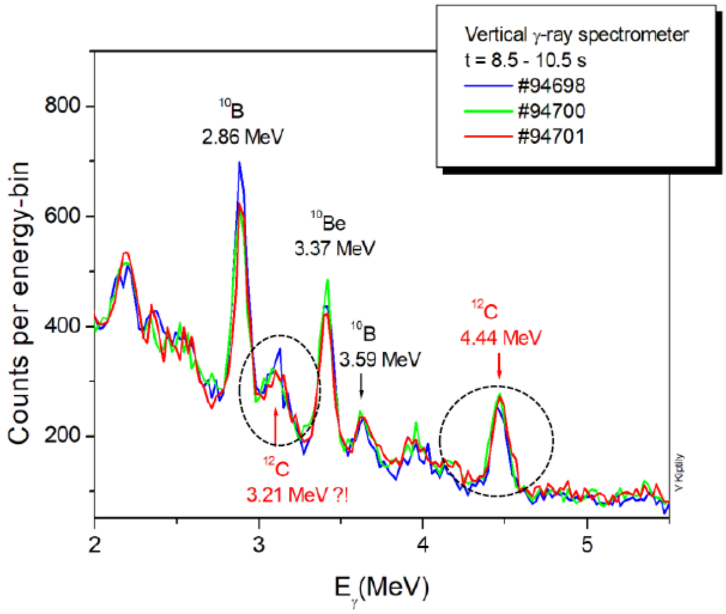

Figure B.2-2: gamma-ray spectrum from the KM6S vertical gamma-ray spectrometer measured in JET discharges #94698, 94700 and 94701 from the 3 ion ICRH experiment M18-11.

For the CeBr3 detector measurements have been performed with using calibration sources (Fig. B.2-3).

Gamma Reference Source

Source no.	AL-2735
Drawing	VZ-1158-001
Dimensions of active surface	Ø 17 mm
Overall dimensions	Ø 27 mm x 0.8 mm
Construction	The radionuclidic mixture is homogeneoulsy distributed onto the active area of the plastic foil. The activated foil is covered on both sides with a paper label and a plastic foil.

Nuclide	Gamma-ray energy [MeV]	Activity [Bq]	Emission rate [s^{-1}]
Americium-241	0.060	3.49E03	1.25E03
Cadmium-109	0.088	1.64E04	5.99E02
Cobalt-57	0.122	5.90E02	5.05E02
Cerium-139	0.166	7.31E02	5.84E02
Mercury-203	0.279	1.39E03	1.14E03
Tin-113	0.392	2.49E03	1.62E03
Strontium-85	0.514	3.06E03	3.02E03
Caesium-137	0.662	2.86E03	2.43E03
Yttrium-88	0.898	5.39E03	5.07E03
Cobalt-60	1.173	3.35E03	3.35E03
Cobalt-60	1.333	3.35E03	3.35E03
Yttrium-88	1.836	5.39E03	5.36E03

Reference date	1 January 2018 at 12:00 UTC
Leakage and contamination test*	Wipe test according to ISO 9978.
Wipe test passed on	4 January 2018
Measuring method	The activity of the source was determined by weighing out calibrated single and/or mixed nuclide solutions. After production the source was verified with a high purity germanium detector with multi-channel analyzer. Temperature during the weighing: 21 °C ± 5 °C
Uncertainty*	The relative uncertainty of the activity is 3 % (Cd-109: 5 %).
Radioactive impurities	Fe-59<1 Bq; Rb-84<1 Bq
Remark	---

* please see HI001

Figure B.2-3: - Specification of the source used in the measurements.

Fig. B2.-4 presents typical recorded spectra. The measurements were performed in the same conditions: the source was placed in front of the scintillator and using a measuring time of 5 minutes. These spectra have been used for the determination of the energy resolution (Table B.2-1).

.

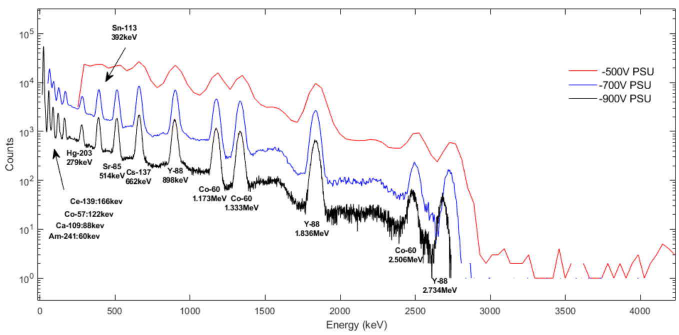

Fig. B2.-4: Spectra registered when using calibration sources

Table B.2-1 – Energy resolution

Nuclide	Energy (keV)	FWHM (%) at -500V	FWHM (%) at -700V	FWHM (%) at -900V
^{203}Hg	279	-	18.23 ± 2.67	16.23 ± 1.66
^{113}Sn	392	-	9.68 ± 0.88	8.09 ± 0.44
^{137}Cs	662	19.61 ± 0.01	6.49 ± 0.83	5.63 ± 0.36
^{88}Y	898	15.99 ± 0.93	5.17 ± 0.53	4.82 ± 0.26
^{60}Co	1173	13.86 ± 1.38	4.17 ± 0.22	3.91 ± 0.13
^{60}Co	1333	10.86 ± 0.64	3.86 ± 0.20	3.61 ± 0.09
^{88}Y	1836	7.14 ± 0.48	3.13 ± 0.11	2.97 ± 0.06
^{60}Co	2506	8.58 ± 1.16	3.20 ± 0.36	3.05 ± 0.23
^{88}Y	2734	4.63 ± 0.13	2.41 ± 0.10	2.02 ± 0.11

C. System Commissioning

The KM6T system has been routinely used during the C38 JET experimental campaign. The spectra acquired during these experiments proved that a significant improvement of the energetic resolution has been obtained. An illustrative example is presented in Fig. C-1 which shows the comparison between the spectra obtained before and after the upgrading. Also is has to be noted that the parasitic neutron capture peak at 2.2 MeV ha been completely eliminated by the neutron attenuator.

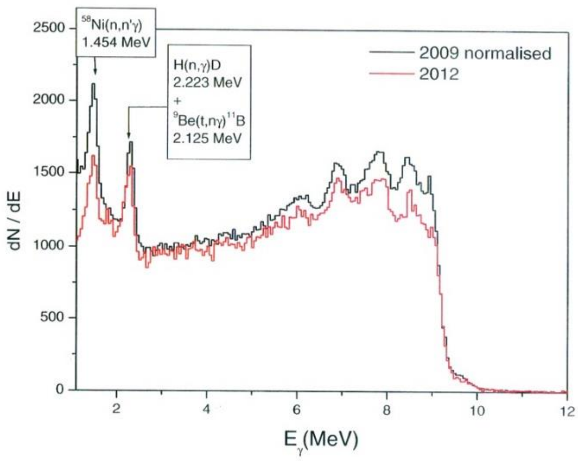

Spectra obtained before the upgrading

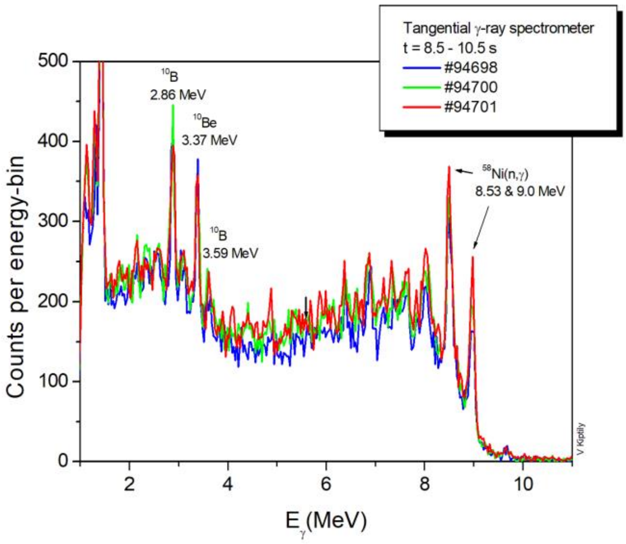

Spectra obtained using upgrading system

Fig. C-1 – Spectra recorded before and after the upgrading

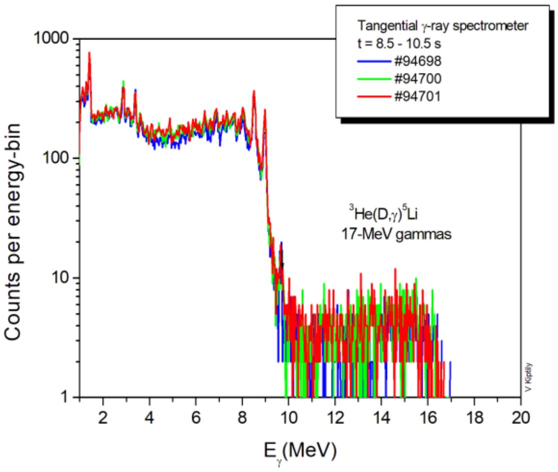

Fig. C-2 - Spectrum showing a clear evidence for the recording of D-^{3}He fusion gamma-rays

Spectra recorded during the M18-12 experiment (SC Massimo Nocente) show a clear evidence for the recording of D-^{3}He fusion gamma-rays (Fig. C-2). This proves that the system is ready for DT fusion measurements.

References:

1. V. Kiptily et al, Fusion Alpha-Particle Diagnostics for DT Experiments on the Joint European Torus, International Conference on Fusion Reactor Diagnostics , Villa Monastero, Varenna (Italy), JET preprint EFDA–JET–CP(13)04/01
2. V.G. Kiptily V.G. Fusion Technology 18 (1990) 583
3. V.G Kiptily. et al. Fusion Technology 22 (1992) 454